JOURNAL OF MATERIALS SCIENCE 29 (1994) 959–964

Microstructure of pressureless-sintered Al_2O_3–24 vol % ZrO_2 composite studied by high-resolution electron microscopy

B.T. LEE, K. HIRAGA, D. SHINDO*
*Institute for Materials Research, and *Institute for Advanced Materials Processing, Tohoku University, Katahira, Aoba-ku, Sendai 980, Japan*

A. NISHIYAMA
Central Research Institute, Mitsubishi Material Co., 1-297 Omiya, Saitama 330, Japan

The microstructure of an Al_2O_3–24 vol % ZrO_2 composite prepared by pressureless-sintering was investigated by high-resolution electron microscopy. The composite was formed of homogeneously dispersed ZrO_2 and Al_2O_3 grains with average sizes of 0.3 and 0.5 μm, respectively. Most ZrO_2 grains had a monoclinic structure, but a few ZrO_2 embedded in Al_2O_3 grains were a tetragonal structure. At interfaces between ZrO_2 with a lamella-type twin structure and Al_2O_3, microcracks were observed, in addition to strain fields in the Al_2O_3 matrix. Complex twin structures accompanied by dislocations were observed in ZrO_2 with a spherical shape. In *in situ* observations with electron-beam heating, it was found that a crack propagated along an Al_2O_3/ZrO_2 interface and stopped at the place where a tetragonal ZrO_2 had undergone a structural change to monoclinic ZrO_2.

1. Introduction

There have been many reports on the development of high strength and high fracture toughness of structural ceramic composites in order to improve their reliability. One of the composites is an Al_2O_3–ZrO_2 system which is known to show phase transformation toughness [1–4]. The Al_2O_3–ZrO_2 composites have been produced for application in the fields of wear parts and tool materials. In these composites, many studies on the fabrication process, microstructures and properties have been performed since 1980 [5–8]. Recently, Al_2O_3 and ZrO_2 powders with higher purity and finer grain size have been produced. Using these powders, Al_2O_3–ZrO_2 composites, which have a higher density and better mechanical properties, have been fabricated by pressureless-sintering at comparatively low sintering temperatures. Although the mechanical properties of these composites have been reported [4, 7, 8], their microstructures have been little investigated.

There have been some studies on the microstructures of ZrO_2 in ZrO_2, Al_2O_3–ZrO_2 and mullite–ZrO_2 systems by transmission electron microscopy (TEM). Bischoff and Rühle [9] studied internal defects and twin structures in monoclinic ZrO_2 (m-ZrO_2) grains in the mullite matrix, and observed mosaic-like structures and sectioned twins, which were induced by the phase transformation during the cooling process. From observations of incoherent interfaces between the Al_2O_3 matrix and dispersed ZrO_2 grains by high-resolution electron microscopy (HREM), Karus-Lanteri *et al.* [10] showed that intergranular ZrO_2 particles are accommodated by ledge and misfit dislocations, depending on the crystallographic orientation of ZrO_2. On the other hand, Mazerolles *et al.* [11] reported that the interfaces of Al_2O_3/ZrO_2 (Y_2O_3) are semicoherent, and they determined the preferred growth directions and epitaxial relationships. TEM observations of martensitic phase transformation and microcracking in tetragonal ZrO_2 (t-ZrO_2) polycrystals containing Y_2O_3 were performed by Wen *et al.* [12] with 200 kV electron-beam irradiation.

The strength and fracture toughness of the composites are considered to depend strongly on the microstructures of grain boundaries and twin structures of ZrO_2 particles in the Al_2O_3–ZrO_2 composites. The purpose of the present work was to investigate the microstructure of the Al_2O_3–24 vol % ZrO_2 composite, which is formed of fine grains of submicrometre size, on the atomic scale using HREM.

2. Experimental procedure

Starting powders with the ratio Al_2O_3–24 vol % ZrO_2 were mixed with a wet ball mill in a plastic jar. After drying in vacuum, the mixtures were pressed at 10 kg mm^{-2}, and then pressureless-sintered for 2 h at 1450° C. The sintered pellets were cut into thin slices using a diamond cutter. The slices were mechanically polished to a thickness of about 150 μm, and 3 mm diameter discs were punched out by an ultrasonic cutter. These disc-shaped samples were polished further to a thickness of about 30 μm thickness by a dimple grinder. The samples were finally thinned with

0022–2461

argon ions at an accelerating voltage of 3 kV with a glancing angle of 25°. The specimens of raw ZrO_2 powders for TEM observations were prepared by dispersing them on holey carbon films. *In situ* observations of crack propagation and phase transformation were performed by rapidly increasing the incident electron-beam intensity. HREM observations were performed using an electron microscope (JEM-4000EX) with a resolution of 0.17 nm.

3. Results and discussion

3.1. Microstructure of Al_2O_3–24 vol % ZrO_2 composite

Fig. 1 shows transmission electron micrograph of the Al_2O_3–24 vol % ZrO_2 composite. ZrO_2 grains, which are observed as relatively dark regions with fine contrast, show nearly homogeneous distribution in the Al_2O_3 matrix. Average sizes of ZrO_2 and Al_2O_3 grains are 0.3 and 0.5 μm diameter, respectively. The grain sizes are extremely small, compared with about 1–2 μm previously reported in pressureless-sintered Al_2O_3–ZrO_2 composites [4–8]. Compared with a grain size of 2.5 μm in Al_2O_3 sintered without ZrO_2 at the same temperature, it can be said that the dispersion of ZrO_2 prevents the grain growth of Al_2O_3. As can be seen, as the dark curved contrast in Fig. 1, strong strain fields in the Al_2O_3 matrix are formed by the spontaneous phase transformation of ZrO_2. The structure and size of ZrO_2 particles depend on the situation of ZrO_2 in the Al_2O_3 matrix. Most of the ZrO_2 particles have a monoclinic structure with various types of twin structures. However, a few ZrO_2 particles embedded in an Al_2O_3 grain, which have a relatively small size and a spherical shape, show a tetragonal structure. An example of this is marked T in Fig. 1. The m-ZrO_2 particle with an ellipsoidal shape, marked M in Fig. 1, shows a complex and sectional twin structure, whereas m-ZrO_2 with a rectangular shape, marked L, shows a lamellar-type twin structure.

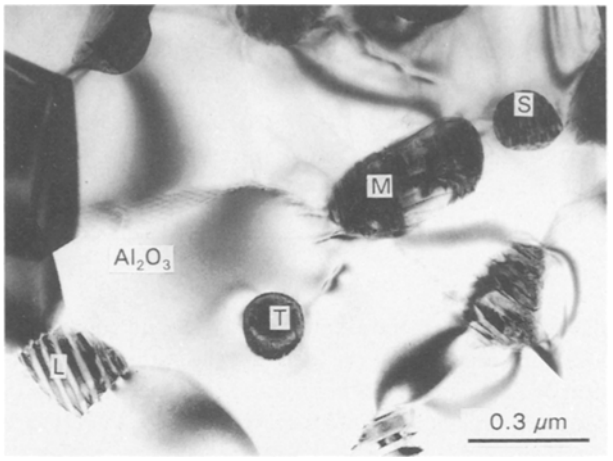

Figure 1 Transmission electron micrograph of an Al_2O_3–24 vol % ZrO_2 composite.

3.2. Structure of the interfaces

It is worthwhile investigating the structure of the interfaces in ceramic composites, in order to understand their mechanical properties. At interfaces between ZrO_2 with a lamellar shape and Al_2O_3, alternate bright and dark contrasts were frequently observed, as can be clearly seen in Fig. 2, where gain L in Fig. 1 is enlarged. These contrasts show the existence of compressive and expansive strain fields in the Al_2O_3 grain, which result from shape and volume changes accompanied by the structural transformation from a tetragonal to monoclinic structure. At this type of interface, microcracks were also observed, as can be seen in Fig. 2, in which the cracks are

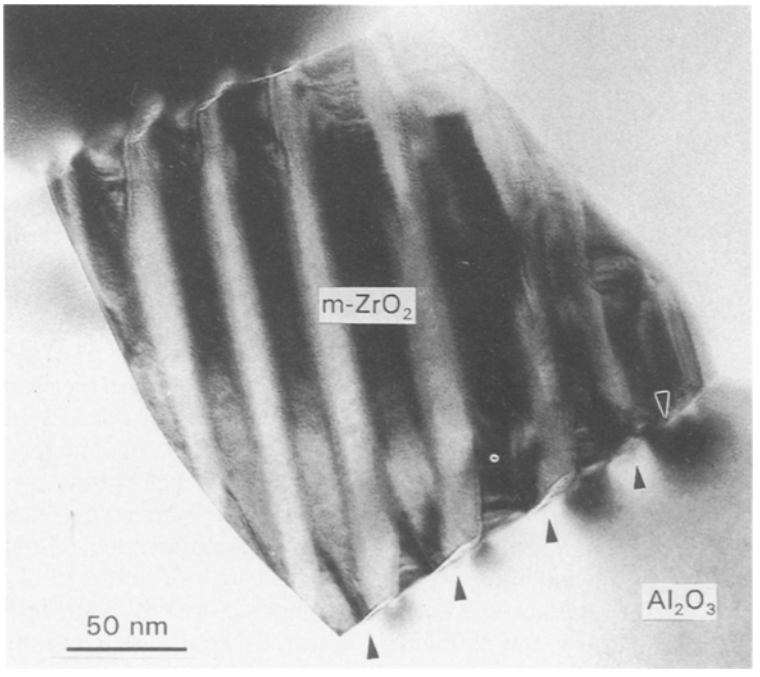

Figure 2 An enlarged micrograph of the m-ZrO_2 marked L in Fig. 1. Arrowheads indicate microcracks.

represented as white streaks, in addition to the strain contrasts in the Al_2O_3 grain, as indicated by arrowheads. The existence of microcracks was also clearly confirmed by HREM.

Fig. 3a shows an HREM image of another interface between a twinned ZrO_2 and an Al_2O_3 grain. In Fig. 3a, periodic white regions can be seen along the interface, as indicated by arrowheads. An enlarged micrograph of the interface marked with a rectangle in Fig. 3a (Fig. 3b) clearly shows the existence of microcracks at the interface. Although the microcrack was covered with an amorphous contamination layer during sample preparation, a gap at the left-hand side can be clearly seen in lattice fringe images in Al_2O_3 and ZrO_2 grains, again indicated by arrowheads.

In a few boundaries between ZrO_2 grains having lamella-type twins, we observed larger cracks. Fig. 4 shows cracks with comparatively large sizes at a boundary between ZrO_2 grains. It is considered that the existence of this type of crack has a detrimental effect on mechanical properties, particularly, fracture strength. Thus, it can be said that the control of grain growth and homogeneous distribution of ZrO_2 particles are important in preventing the appearance of this type of crack.

On the other hand, the interfaces between ZrO_2 with no twin structure and Al_2O_3 are joined without any impurity phases, as shown in the HREM image of Fig. 5. That is because the composite was synthesized with high-purity Al_2O_3 and ZrO_2 powders without any sintering agents. The boundary in Fig. 5 is a small-angle semi-coherent interface, in which a (1 0 0) plane of ZrO_2 and (0 1 2) of Al_2O_3 make an angle of about 8°. There are no deformations of lattice fringes along the B–C boundary parallel to a (1 0 0) plane of ZrO_2, whereas a semiperiodic array of disturbed regions, like dislocations, indicated by arrowheads, are observed along the A–B boundary.

3.3. Twin structure of ZrO_2

In order to compare with ZrO_2 in the Al_2O_3–ZrO_2 composite, raw ZrO_2 powders were examined first. Most of the raw ZrO_2 powders have fine sizes less than 0.1 μm. An HREM image taken with the incident beam parallel to the [0 $\bar{1}$ 1] direction is shown in Fig. 6, together with an electron diffraction pattern. The monotonic contrast of this crystal shows that this powder has a disc-like shape. It was found from TEM observations that most ZrO_2 powders have disc-like shapes. The HREM image and electron diffraction pattern show a typical monoclinic structure with

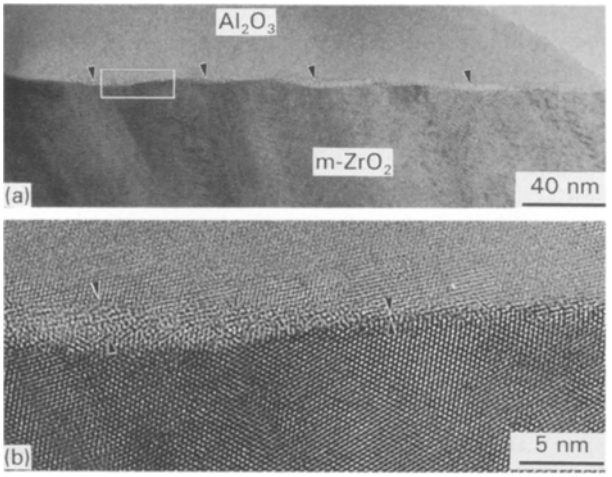

Figure 3 HREM image of an Al_2O_3/ZrO_2 interface with microcracks, indicated by arrowheads in (a). (b) Enlarged micrograph of the region within the rectangle. A microcrack was covered with an amorphous contamination layer during sample preparation.

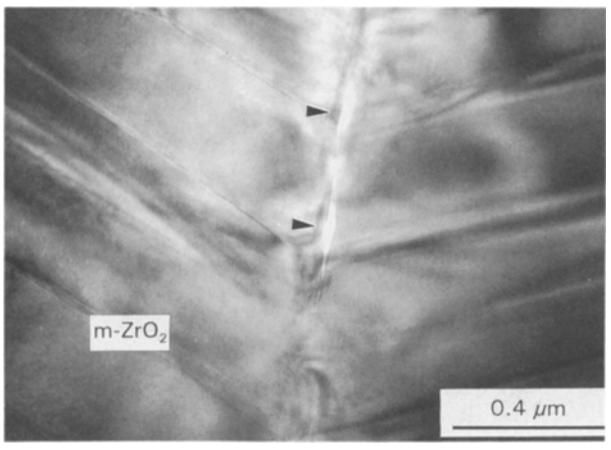

Figure 4 Transmission electron micrograph of a grain boundary of ZrO_2 having lamellar-type twins. Arrows indicate large cracks.

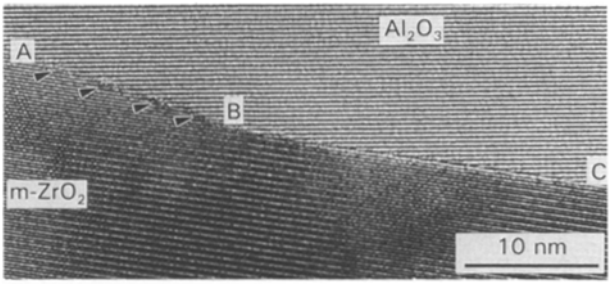

Figure 5 HREM image of an interface between Al_2O_3 and ZrO_2 with no twin structure.

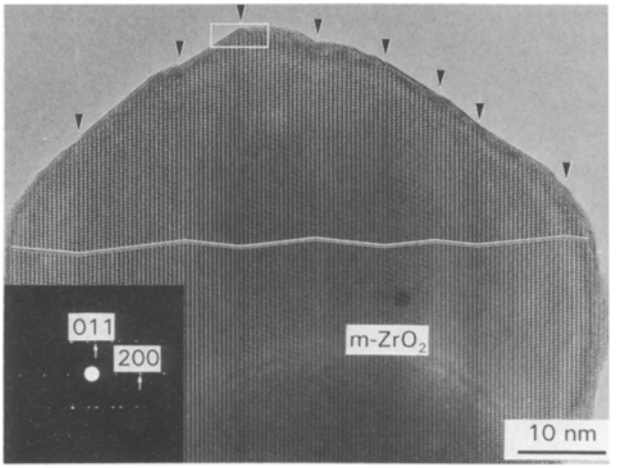

Figure 6 HREM image and diffraction pattern of m-ZrO_2 raw powder, taken with the incident beam parallel to the [0 $\bar{1}$ 1] direction. Arrows indicate twin boundaries.

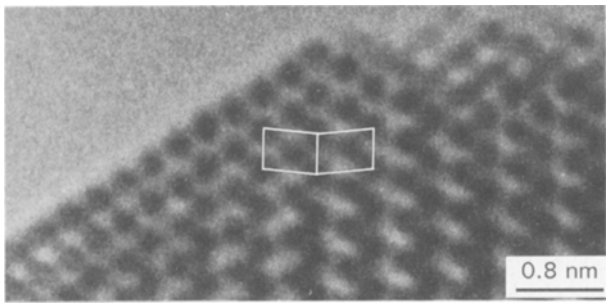

Figure 7 Enlarged micrograph of the thin region within the rectangle in Fig. 6. Two parallelograms show unit cells with a twin relationship.

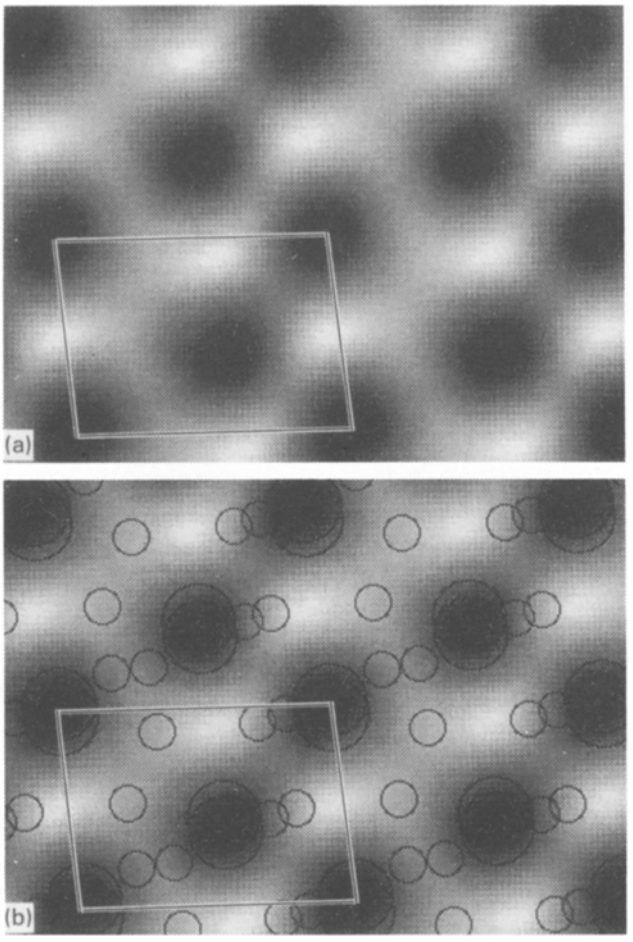

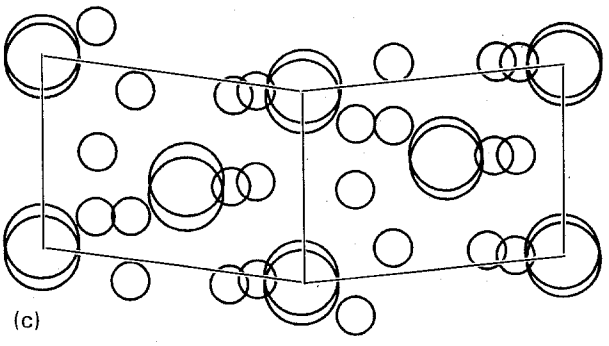

Figure 8 (a) Calculated HREM image of m-ZrO_2 with a thickness of 5 nm and a defocus value of -45 nm. (b) Projected atomic arrangement superimposed on the calculated image. Large and small circles correspond to zirconium and oxygen atoms, respectively. (c) Structure model of (1 0 0) twin, determined from the calculated (a) and observed (Fig. 7) images.

(1 0 0) twin planes. An atomic arrangement across the (1 0 0) twin plane may be determined from image contrast in a thin region near the edge of the crystal. Fig. 7 is an enlarged image of the thin region within the rectangle in Fig. 6. From a calculated image and an atomic arrangement superimposed on the image in Fig. 8a and b, it can be said that dark dots in the observed image of Fig. 7 correspond to double zirconium atom positions. From the calculated image and the observed image contrast around the (1 0 0) twin plane in Fig. 7, a structural model at the (1 0 0) twin is proposed as in Fig. 8c, although there is ambiguity for an arrangement of oxygen atoms. In the model, one notices that the atomic arrangement does not have a mirror relationship across the twin plane, and is formed by shear stress.

Most of all raw ZrO_2 powders have twin structures formed with straight (1 0 0) twin planes without any steps and with no stacking faults, as shown in Fig. 6. The simple twin structure will be compared with twin structures of ZrO_2 in the Al_2O_3–ZrO_2 composites. Fig. 9 is an HREM image of ZrO_2 with a typical lamellar-type twin structure in the composite, together with an electron diffraction pattern. The HREM image of Fig. 9a, taken with the electron beam parallel to the [0 1 0] direction, shows the (1 0 0) twin planes and stacking faults. The enlarged micrograph of Fig. 9b clearly shows twin relationships across the (1 0 0) planes by lattice fringes.

The HREM image of Fig. 10 shows the microstructure of the other ZrO_2 particle. In the micrograph, $(\bar{3}\,0\,2)$ twin boundaries and many planar defects, such as stacking faults, which seem to be slightly tilted from the incident electron beam, were observed. Lattice fringes show the existence of many edge-type dislocations, as marked with black circles.

Fig. 11 shows an HREM image of ZrO_2 with a spherical shape, placed at an Al_2O_3 grain boundary, marked S in Fig. 1. In the image, a complex twin structure is seen, which is different from the simple twin structures in Figs 9 and 10 which have lamella-

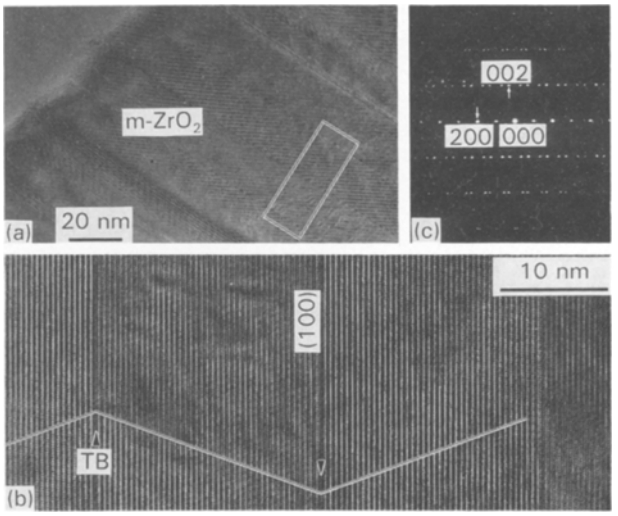

Figure 9 (a) HREM image of twinned m-ZrO_2 and (c) the electron diffraction pattern. (b) Enlarged micrograph of the region within the rectangle in (a).

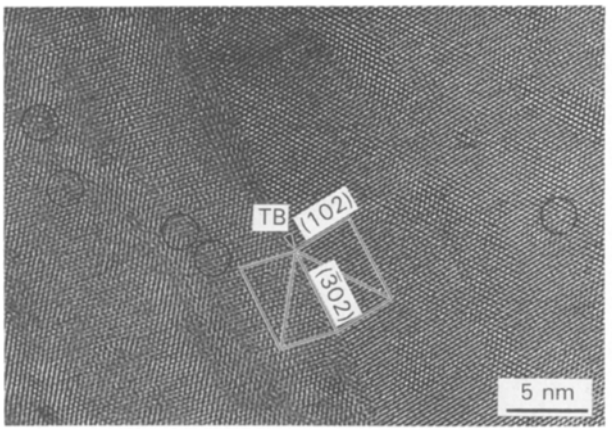

Figure 10 HREM image of m-ZrO_2 showing ($\bar{3}$ 0 2) twin boundaries, and planar defects and dislocations. Some dislocation cores are circled.

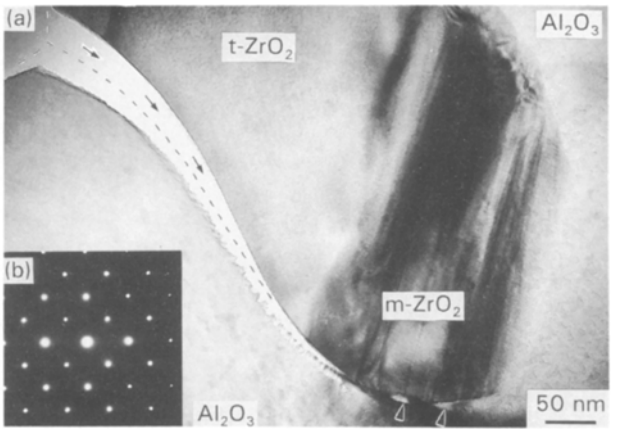

Figure 12 (a) *In situ* observation of crack propagation along an interface of t-ZrO_2/Al_2O_3, and of t–m transformation at the crack tip. (b) Electron diffraction pattern of t-ZrO_2.

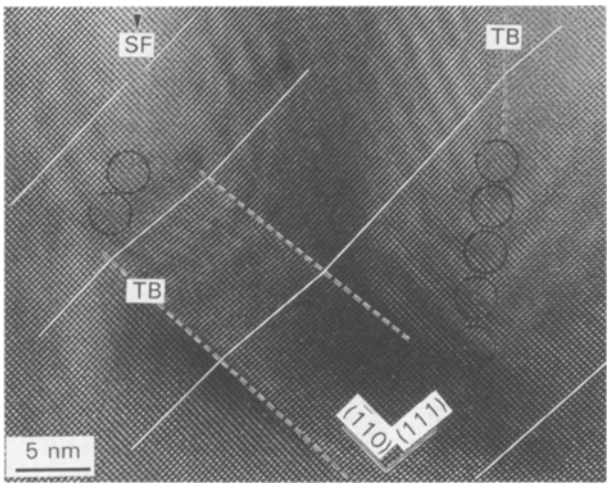

Figure 11 HREM image of m-ZrO_2 showing complex twin structures. Twin boundaries (TB), indicated by dotted lines, and a stacking fault (SF), disappear halfway inside the grain, accompanied by some dislocations marked with black circles.

type twin structures. Because the t–m phase transformation occurred under strong constraint from surrounding Al_2O_3 crystals, anisotropic volume change is restricted. In Fig. 11, the disappearance of twin boundaries, which was accomplished by the appearance of many edge-type dislocations, in order to avoid the generation of a directional volume change, were observed, as indicated by dotted lines.

3.4. Crack propagation by electron-beam heating

Evidence of phase transformation of a dispersed t-ZrO_2 particle was sought using electron-beam heating. In the initial stage of electron-beam irradiation, only notch was observed at the end of an Al_2O_3/ZrO_2 interface, shown by dotted lines in Fig. 12, and also this intragranular ZrO_2 had a tetragonal structure as shown in the electron diffraction pattern. After electron-beam heating for several times, it was observed that a crack slowly propagated along the Al_2O_3/ZrO_2 interface, and then was stopped by the t–m phase transformation which occurred at the crack tip, as shown in Fig. 12. Twin bands, resulting from the phase transformation, produce compressive and expansion strain fields along the interface, as indicated by arrowheads in Fig. 2. The energy of the crack propagation may be interpreted as being reduced by the appearance of the strain fields.

4. Conclusions

The microstructure of the Al_2O_3–24 vol % ZrO_2 composite, which was prepared by pressureless-sintering at 1450° C using high-purity, fine raw powders of Al_2O_3 and ZrO_2 was characterized as follows.

1. The composite is formed by a homogeneous distribution of Al_2O_3 and ZrO_2 with average sizes of 0.5 and 0.3 μm, respectively.
2. Most ZrO_2 particles in the composite have a monoclinic structure, but a few, embedded in Al_2O_3 grains, have a tetragonal structure.
3. Twin structures of m-ZrO_2 grains are mainly divided into two types, simple lamella-shaped and complex ones.
4. ZrO_2 with a lamella-shaped twin structure produces compressive and expansive strain fields in the adjoining Al_2O_3 matrix and microcracks at the interface with Al_2O_3.
5. ZrO_2 with a spherical shape shows complex twin structures in order to avoid anisotropic shape change in the t–m phase transformation. In the structures, many twin boundaries disappear halfway inside the grain, by generating dislocations.
6. Interfaces between Al_2O_3 and ZrO_2 with no twins are joined without any impurity phase.
7. By electron beam heating, crack propagation along an interface of Al_2O_3/ZrO_2 and t–m phase transformation at the crack tip were observed.

References

1. A. G. EVENS, N. BURLINGAME, M. DROY, and W. M. KRIVEN, *Acta Metall.* **29** (1981) 447.
2. F. F. LANE, *J. Mater. Sci.* **17** (1982) 247.
3. P. F. BECHER, *J. Am. Ceram. Soc.* **64** (1981) 37.

4. H. SABURO, Y. MASASHIRO, and S. SHIGEYUKI, *ibid.* **69** (1986) 169.
5. N. CLAUSSEN, J. STEEB, and R. F. PABST, *J. Am. Ceram. Bull.* **56** (1977) 559.
6. D. J. GREEN, *J. Am. Ceram. Soc.* **65** (1982) 610.
7. S. R. WITEK, and E. P. BUTLER, *ibid.* **69** (1986) 523.
8. Q. L. GE, T. C. LEI and Y. ZHOU, *Mater. Sci. Technol.* **7** (1991) 490.
9. E. BISCHOFF, and M. RÜHLE, *J. Am. Ceram. Soc.* **66** (1983) 123.
10. S. P. KRAUS-LANTERI, T. E. MITCHEL, and R. PORTIER, *ibid.* **69** (1986) 256.
11. L. MAZEROLLES, D. MICHEL, and R. PORTIER, *ibid.* **69** (1986) 252.
12. S. L. WEN, L. T. MA, J. K. GUO, and T. S. YEN, *ibid.* **69** (1986) 576.

Received 9 November 1992
and accepted 26 August 1993